Journal of Marine Science and Technology

Volume 23 | Issue 3 Article 1

INNOVATIVE ASPHALT RESEARCH USING ACCELERATED PAVEMENT TESTING

Manfred N. Partl
Swiss Federal Laboratories for Materials Science and Technology, Empa, Duebendorf, Switzerland.,
manfred.partl@empa.ch

Christiane Raab
Swiss Federal Laboratories for Materials Science and Technology, Empa, Duebendorf, Switzerland.

Martin Arraigada
Swiss Federal Laboratories for Materials Science and Technology, Empa, Duebendorf, Switzerland.

Journal of Marine Science and Technology, Vol. 23, No. 3, pp. 269-280 (2015)
DOI: 10.6119/JMST-014-0326-1

INNOVATIVE ASPHALT RESEARCH USING ACCELERATED PAVEMENT TESTING

Manfred N. Partl, Christiane Raab, and Martin Arraigada

Key words: accelerated pavement testing (APT), model mobile load simulator (MMLS3), mobile load simulator (MLS10).

ABSTRACT

Accelerated pavement testing is one key for innovations in the field of road pavement structures and materials due to its power of assessing mechanical performance in close to reality situations. This paper discusses two types of mobile load simulators for applying unidirectional wheel loads at comparatively high frequencies, the MMLS3, a one third scale device, and the MLS10, a full-scale device. Through examples it is demonstrated that these devices are suitable for testing complex systems, such as mechanical resistance of light reflectors on pavements, traffic resistance of bituminous plug expansion joints for bridges, performance of grid reinforced pavements as well as water resistance of porous asphalt against traffic induced pumping effects. Moreover, an example of MLS10 ultimate bearing capacity tests on a real test section is shown focusing on the discussion of strain gauge, acceleration, rut depth and falling weight deflectometer (FWD) measurement results.

I. INTRODUCTION

Traffic load simulators of different dimensions, characteristic and design have been used effectively for more than 50 years. Their application is driven by the need for accelerated and close to reality testing of pavement innovations in terms of materials, road structures and installation techniques. They help to minimize the risk of expensive development failures and to adapt the quality standards to constantly increasing needs and demands. Furthermore, their application allows to determine the influence of new developments in motor vehicle construction and to evaluate the effect of changing loads on the structural behavior of pavement constructions in a reasonably rapid way.

Besides of allowing faster mechanical performance predictions of road pavements, the advantage of such traffic load simulators originates in the fact that they allow for reproducible, clearly defined testing procedures. Some of them are even mobile and can be used on real test sections with minimal obstruction of the normal traffic flow. In combination with sophisticated test setups and modern measurement technology, they enable retrieving significant information for better understanding of the system including more reliable input for system and materials evaluation as well as structural design models.

Nevertheless, it cannot be ignored that only the effect of mechanical loading can be evaluated in an accelerated way, for example by increasing the number of stress cycles or load amplitudes, while time lapse effects of climate influences or aging processes are difficult to simulate.

Many of the currently available traffic simulators, stationary or mobile, are prototypes or exist only in a limited number. Their acquisition, operation and maintenance is therefore subjected to relatively high costs and significant human resources, including a high percentage of well-trained and specialized staff. Consequently, the existing systems range from very small scale APT devices to stationary full scale facilities, with circular, elliptic and linear test tracks, or mobile full scale machines with linear wheel loading systems. More unusual are stationary full scale facilities, constructed as centrifuges with mantle wheels or with wheels running in a narrow radius or rotating around a vertical axis.

At Empa, the Swiss federal laboratories for material science and technology, actually two accelerated traffic load simulators are in use: the small scale Model Mobile Load Simulator MMLS3 with 300mm tires and the large scale Mobile Load Simulator MLS10 with realistic double or single tires.

In the following both traffic simulators and their application for innovative asphalt pavement research are presented.

II. THE MODEL MOBILE TRAFFIC LOAD SIMULATOR MMLS3

1. Device and Operating Principle

The MMLS3 (Model Mobil Load Simulator) is a laboratory 1:3 scaled device. It consists of a stiff metal frame (2400 mm × 600 mm × 1150 mm) and four height-adjustable feet (see Fig. 1). The load is applied through four single tires

Paper submitted 11/30/13; revised 12/23/13; accepted 03/26/14. Author for correspondence: Manfred N. Partl (e-mail: manfred.partl@empa.ch).
Swiss Federal Laboratories for Materials Science and Technology, Empa, Duebendorf, Switzerland.

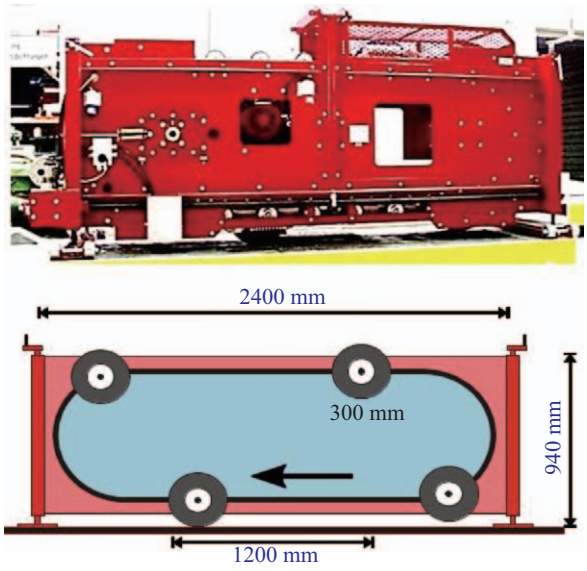

Fig. 1. MMLS3 device and operating principle.

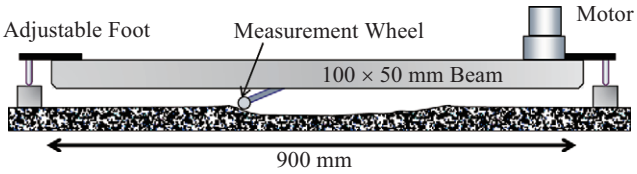

Fig. 2. Profilometer, operating principle.

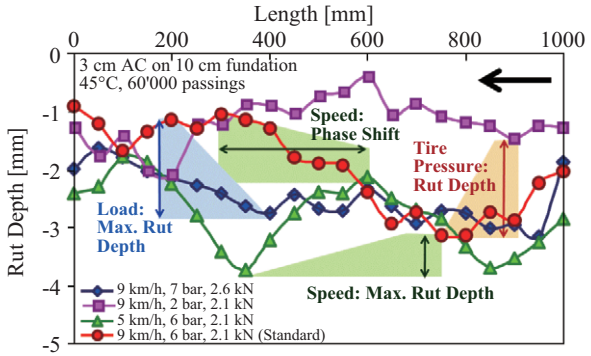

Fig. 3. Longitudinal deformation in the wheel path for different speeds and tire pressures.

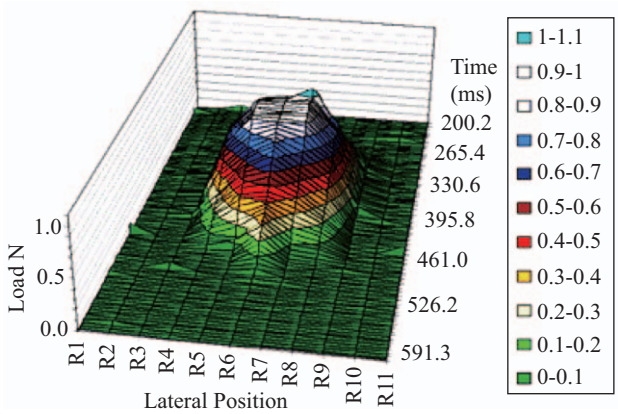

Fig. 4. Contact pressure distribution under MMLS3 wheel.

(diameter: 300 mm, width: 80 mm) running in one direction on a guide rail comparable to a chain saw. The machine allows approximately 7200 load applications per hour which corresponds to a speed of 9 km/h. The longitudinal distance between two tires is 1260 mm. The load on the wheels can be adjusted with springs between 1.9 kN and 2.7 kN and the tire pressure can be varied between 560 kPa and 800 kPa. The machine is used for accelerated testing in situ and in the laboratory in order to determine the mechanical resistance of flexible pavements under rolling wheel loads against crack formation and, in particular, rutting and permanent deformation of surface courses (Gubler et al., 2004; Raab et al., 2005; Sokolov et al., 2005; Hean and Partl, 2008; Kim et al., 2009; Raab et al., 2011).

For the measurement of permanent deformation, a special profilometer with a maximal range of 40 mm is used (Fig. 2). The profilometer consists of a measurement beam which is bridging the profile while supported on two fix reference points. Alongside the measurement beam a spring arm driven by a step motor, presses a 25 mm wheel against the pavement surface. While travelling along the pavement surface the movement of the spring arm is recorded with a linear displacement transducer and converted via an electronic data acquisition system into an image of the surface profile providing quantitative information about the rutting.

Comparative measurements on a 3 cm asphalt concrete parking lot pavement with a nominal surface temperature of 45°C show that the longitudinal deformation after 60'000 wheel passings notably depends on speed and tire pressure (Fig. 3). This is true in particular for the outgoing half of the wheel track. Different speeds influence the maximum rut depth and may produce a longitudinal phase shift. Lower tire pressures have a positive impact on the longitudinal profile. Higher loads and pressure increase the maximal rut depths and change the longitudinal profile as well. Therefore, the speed of loading, the contact pressure and the tire pressure are very important for MMLS3 testing. Generally, the contact pressure distribution seems to be quite constant as shown in Fig. 4.

The MMLS3 tests can be conducted at a maximal environmental temperature of 45°C (climatic chamber or heated tent). It is also possible to heat up the road surface with a special fan consisting of two alternating flat nozzles for producing temperatures up to 60°C. When using a climatic chamber it is possible to evaluate the pavement performance in the laboratory under a constant temperature distribution over the whole cross section of the pavement. This procedure is very convenient for system analysis in the frame of screening tests of large flexible asphaltic plug expansion joints for large horizontal bridge movements since the stability of the bearing

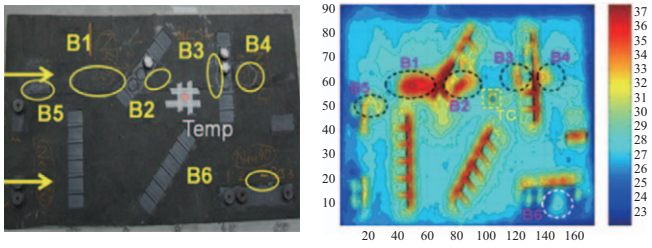

Fig. 5. Visual and thermal images of reflectors after MMLS3 tests, debonding occurred at ring markings, arrows show traffic direction.

Fig. 6. MMLS3 field testing of bituminous plug expansion joints in a heated tent.

structure and the adhesion between plug expansion joint and pavement is more critical for the isothermal case than in case of temperature gradients. In contrast, the use of the special fan or the heated tent is advisable mainly for in situ testing, when a given installation is evaluated regarding quality and performance characteristics.

In the following some examples of MMLS3 testing are presented.

2. Functionality of Light Reflectors

Light reflectors such as used for additional safety at pedestrian crossings are glued to the road surface and therefore subjected to complex mechanical loadings. In order to achieve durable and reliable functioning of these reflectors, the mechanical behavior of the road reflectors themselves, as well as the contact zone between the reflectors and the road surface under alternating wheel loading plays a critical role.

The verification of the functionality of such reflectors has to be done close to realistic traffic loads and therefore MMLS3 was used (Sokolov et al., 2005). The investigated reflector system consisted of a reflector which was attached to the pavement surface with special two-component glue. For testing, the reflector was glued on both old and new asphalt concrete slabs and evaluated at two different elevated constant temperatures 30°C and 40°C. Each slab was trafficked on both the left and right side. It was observed that the contact zone between the reflector and surface of the new specimen was destroyed in the rutting zone only after some thousand wheel passings. In order to determine the position and shape of debonding zones on the tested specimen, infrared (IR) thermography measurements were carried out (Fig. 5). Additionally, the resistance to temperature cycles was tested on an old compacted asphalt pavement specimen with the aim to investigate the adhesive behavior of the reflectors and cover material after 20 temperature cycles. It was found, that temperature has an important influence on the adhesion and that adhesion significantly dependents on the surface properties of the pavement. While the reflector system on an old asphalt pavement with a comparatively high amount of uncoated aggregate on its surface showed very promising results, the reflector system on a new asphalt pavement with a comparatively high amount of coated aggregate on its surface suffered debonding failures.

3. Performance Evaluation of Bituminous Plug Expansion Joints

Flexible bituminous (or "asphaltic") plug expansion joint systems are used for short concrete bridges with small maximal horizontal total movements in each joint of about 30 mm for more than 20 years and, recently, even for bridges with large joint movements in the order of 100 mm. As compared to other systems such as conventional steel systems, these plug joints generally have a shorter life cycle. However, they are easy to install, maintain and repair, provided that work is conducted carefully with sound technical know-how and under favorable weather conditions (dry and warm).

Asphaltic plug joints are mostly used in combination with asphalt bridge deck pavements providing a smooth driving surface with positive effect on traffic noise reduction and driving comfort for cars, motor cycles and bikes. In fact, the potential of noise reduction is one of the main advantages of this type of plug joint for bridges in heavily populated urban areas and in critical places such as exposed bridges in alpine nature reserves and recreational areas.

Since plug joints are special multifunctional bridge deck pavement elements with potentially high impact on traffic safety (skid resistance, evenness, potholes from material loss) and durability of the bridge structure, they must be carefully evaluated and tested with respect to their performance. Rutting performance evaluation of such systems is possible in the laboratory and in the field using MMLS3.

On-site investigations of the rutting resistance of the plug joints within and between the wheel paths were conducted with the MMLS3 as shown in Fig. 6 (Partl and Hean, 2011). MMLS3 testing was performed in a tent at 30°C measured 20 mm below surface.

The results depicted in Fig. 7 show that except for "MMLS-3", with partly renewal of the plug joint, all rut depths after 6'000 wheel passings remained clearly below the required 5 mm, i.e. in the order of 3 mm. From this result one can conclude that partial renewal of the plug joint surface material can only be considered as a temporary solution and should be evaluated very carefully.

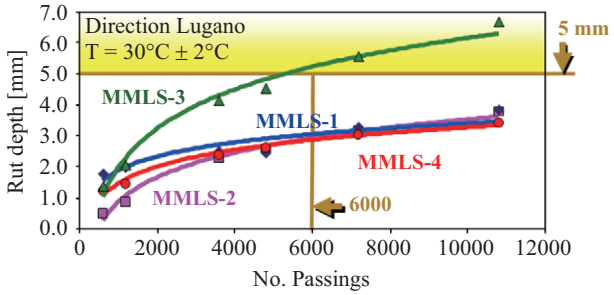

Fig. 7. Rutting results after MMLS3 testing.

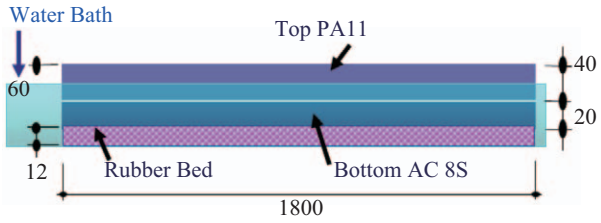

Fig. 8. Rutting results after MMLS3 testing.

Fig. 9. Rutting results after MMLS3 testing.

4. Water Resistance of Porous Asphalt Surface Courses

In addition to stresses and strains from traffic and climatic loading, open graded porous asphalt surface courses PA are extremely exposed to the effects of water flowing through their pores. In order to simulate the pumping effect caused by traffic induced loading and to evaluate the mechanical load bearing capacity of such surface courses MMLS3 tests were conducted (Kim et al., 2009). For this purpose, a special test set-up was chosen. A two layered model pavement slab consisting of 20 mm asphalt concrete AC 8 and 40 mm mastic asphalt PA 11 on top was constructed. This model pavement was put on a rubber mat and tested dry as well as emerged under water of 25°C up to 20 mm below the pavement surface (Fig. 8).

While failure under dry conditions only appeared after 320'000 wheel passings, the load bearing capacity under wet condition was already at a limit after 230'000 cycles due to heavy stripping of the binder as shown in Fig. 9.

5. Performance of Reinforced Pavements

Reinforcement of asphalt pavements has become a valuable tool for preventing reflective cracking and prolonging service life of asphalt pavements. Although the overall advantage of reinforcement seems beyond doubt, there is still disagreement within the road owners on its effectiveness and bonding performance. Reinforcement interlayers are often applied to prevent asphalt pavement overlays from reflective cracking induced by the damaged concrete below. Hence, producers of reinforcements must demonstrate the capability of their products to prevent reflective cracking and to prolong the service life of pavement structures. For this purpose MMLS3 test were conducted comparing two different types of glass fiber reinforcements and one non-reinforced structure.

In order to compare the long-term crack resistance of non-reinforced and grid reinforced pavements in the laboratory, model pavement slabs 435 mm × 1800 mm with two layers of 30 mm asphalt concrete AC 8 were constructed. For the reinforced slabs, glass grids were placed between the layers. Grid #1 was a fiberglass reinforcement grid consisting of glass fiber strands, arranged in a grid structure and covered with a polymer adhesive. Grid #3 was also a fiberglass reinforcement with modified polymer coating and bonded to a spun bond polyester textile (felt) specifically engineered for asphalt overlays. After construction, all 3 slabs were turned upside down and two artificial cracks of about 3 mm width and 25 mm depth were cut along the total width of the slab in a distance of 190 mm symmetrical to the middle of the slabs as shown in Fig. 11.

The slabs were installed in a shed which allowed for a controlled temperature situation. The slabs were put on two supports in a distance of 175 mm from each end on top of a concrete plate. In the middle a thin rubber mat was placed. The failure of the slabs was expected to be caused by cracking and/or delamination during the traffic simulation. It was expected that due to the progression of cracking the stiffness of the slabs was going to decrease, leading to an increase in their bending deformation. Therefore, 6 deformation sensors were installed as visible in Fig. 10 in order to monitor the development of cracking. Fig. 11 shows the whole test setup schematically.

Tests were performed at 20°C measured with a temperature sensor at the interface in the center of the slab. During testing, the temperature in the slabs increased by about 5°C due to the movement of the machine (Fig. 13). The tests were stopped during the night to avoid damage in case of failure of the slab. The tests for the individual slabs were run until failure (cracks, debonding) was observed. Measurements of the deflection of the slab were recorded every five minutes. The length of each file record was set to 30 seconds that includes approximately 60 MMLS3 wheel passings. For each file, the average deflection was calculated, together with the measured temperature and the number of wheel passings at which the file was recorded.

Fig. 12 shows one record containing the deformation measured with deformation sensors WA4 (position 4), WA5 (position 5) and WA6 (position 6) for each passing of the MMLS3. The timestamp of the measurement as well as the recorded

Fig. 10. MMLS3 with deformation sensors.

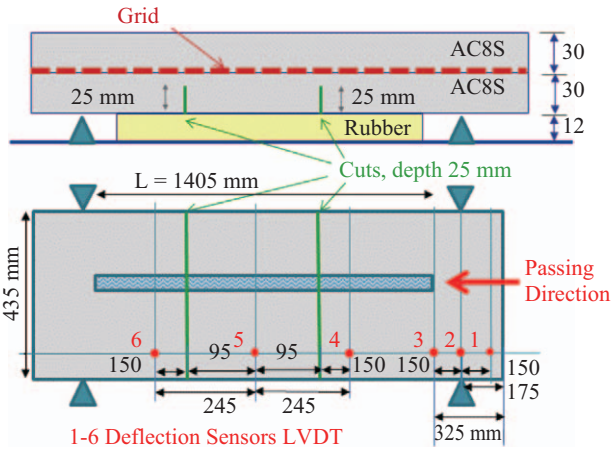

Fig. 11. Schematic of test set-up.

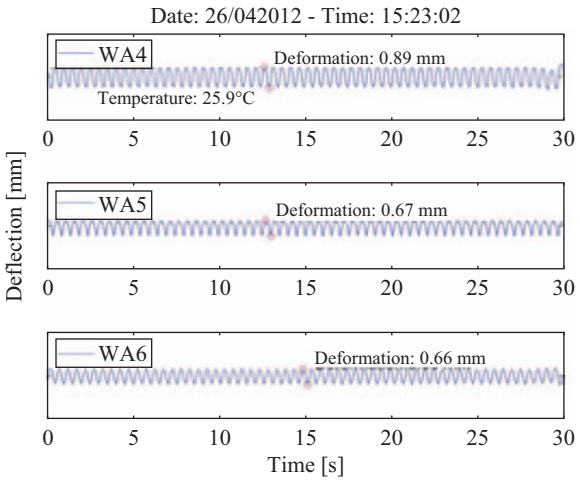

Fig. 12. Measured deflection.

temperature and the calculated deformation are also included in the Figure. This confirms the data in Fig. 3 where for standard loading a higher loading in the incoming half of the wheel track was found.

From each of the records, the average deformation vs. the number of MMLS3 passings was calculated. Fig. 13 shows

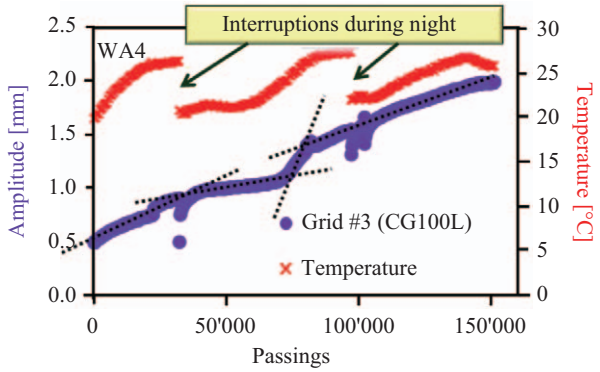

Fig. 13. Average deformation and temperature *vs.* MMLS3 passings (deflection was shifted to eliminate the influence of temperature and healing on the results).

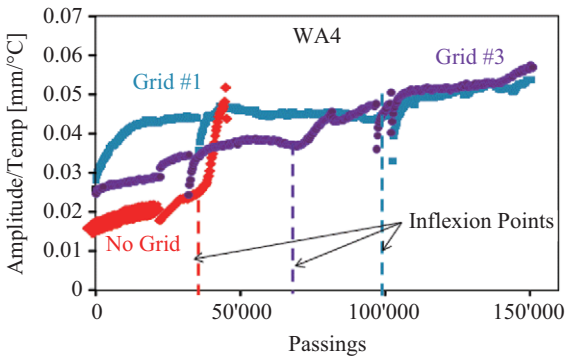

Fig. 14. Average deflection of each slab *vs.* MMLS3 passings.

the deformation for slab 3 with Grid #3 until failure as an example. In the same figure, the temperature is plotted on the secondary axis.

Tests were performed at 20°C measured in the center of the slab. During testing the temperature in the slabs increased by about 5°C due to the continuous internal friction of the slab induced by the MMLS3 passings. As a consequence, the stiffness of the slab and pavement deformation increased. Additionally, Fig. 13 illustrates the effect of the interruptions of the tests during night stops, showing a discontinuity of the measured temperature and the calculated deflection.

In order to reduce the influence of temperature change on the growth of the deflection of the slab, the quotient between the deflection and temperature was calculated and defined as temperature compensated deflection amplitude. Since the temperature differences were so small, this simplified compensation was considered acceptable. The units of the compensated deflection amplitudes have no physical meaning. Fig. 14 showsthese amplitudes as a function of wheel passings calculated for each slab at position 4 (sensor WA4). A constant slope means a stationary change of stiffness without any significant damage. A sharp change in the slope of the quotient can be understood as a sudden change in the slab stiffness, for example as result of crack propagation. For each curve, an

Table 1. MMLS3 passings until reaching the loading limit.

Slab No	reinforcement	MMLS3 passings until loading limit
1	no reinforcement	30'000
2	Grid #1	97'000
3	Grid #3	65'000

inflexion point was identified at the beginning of the failure phase and the number of passings at this point was considered as loading limit.

Table 1 summarizes the number of passings until reaching the loading limit of each slab. The visual inspection confirmed that the appearance of cracks was consistent with the results of the table. Since all slabs were loaded the same way, it was possible to classify the slabs in terms of traffic resistance, showing that slab 2 with Grid #1 was the most resistant and the slab with no grid was the weakest.

According to the test results, the resistance of slab 2 with Grid #1 is approximately 3 times higher than the resistance of the non-reinforced slab whereas the resistance of slab 3 with Grid #3 is twice as high as the resistance of the slab without reinforcement.

The differences between the two reinforcement grids might be caused by their different structure. The different behavior of the two grids can be attributed to the negative impact of the polyester felt of Grid#3 on the interlayer bonding properties, leading to accelerated crack propagation and premature failure.

Visual inspection showed that failure in all slabs was caused by vertical crack propagation. For the non-reinforced slab the crack propagated through the whole specimen leading to total damage (slab fell apart). In case of reinforced slabs crack propagation was delayed and when it appeared it eventually led to delamination and dynamic debonding of the layers. Hence, in both cases it was not possible to take cores and perform Leutner interlayer shear tests. Figs. 15 to 17 show the failure mode for the different slabs.

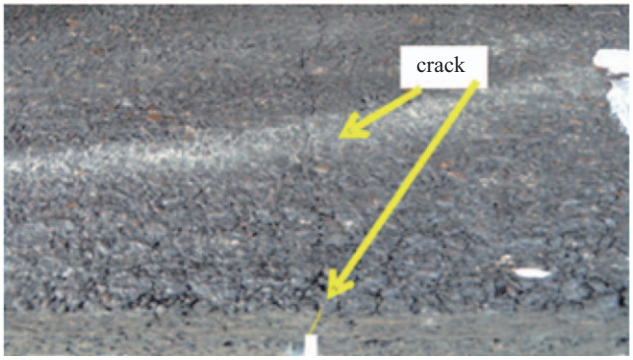

Fig. 15. Failure caused by vertical crack propagation (slab 1 without reinforcement).

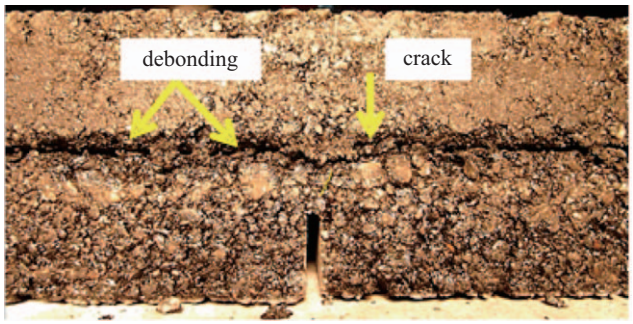

Fig. 16. Failure caused by vertical crack propagation and debonding (slab 2 with Grid #1).

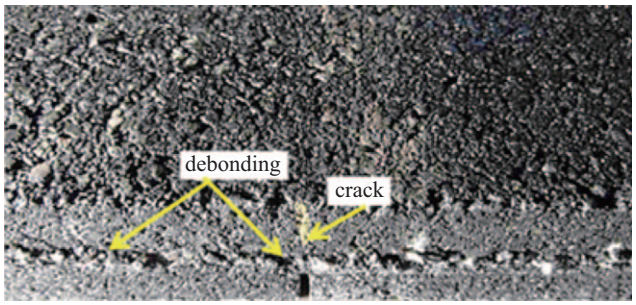

Fig. 17. Failure caused by vertical crack propagation and de-bonding (slab 3 with Grid #2).

III. THE MOBILE LOAD SIMULATOR MLS10

1. Device

The MLS10 is a machine that simulates full-scale truck loading on pavements. The operation principle is similar to that of the MMLS3. The machine loads the pavement with unidirectional tire passings in a length of about 4.2 m, simulating the load of half an axle of a truck. The rolling speed of the tires can go up to 22 km/h, reproducing the passing of up to 6000 half axles per hour. A hydro-pneumatic suspension system allows setting the loads applied by the tires up to 65 kN, corresponding to a 130 kN axle load. The MLS10 and can be equipped with single and dual tires.

The MLS10 has a total weight of 32t and essentially consist of a steel frame made of two large vertical iron plates connected through four robust tanks of about 2 m length and 1 m in diameter, thus creating a very stiff frame for the whole system. One of the tanks is used for water storage and the other three for diesel, each having 1300 liter capacity. This provides additional ballast and allows operating the on-board diesel engine of the machine for about 300 h without refueling. The engine is coupled with a generator that delivers the required power of 50 kW/h for a fully autonomous operation of the machine. Attached to the internal face of the frame plates are two pairs of guide rails that form a closed loop path, like a chain saw.

The tires for loading the pavement are mounted in four bogies, which are strong steel framed carriages that are assembled to a chain rolling along the guide rails. The four bogies of the MLS10 have steel wheels that fit within the rails.

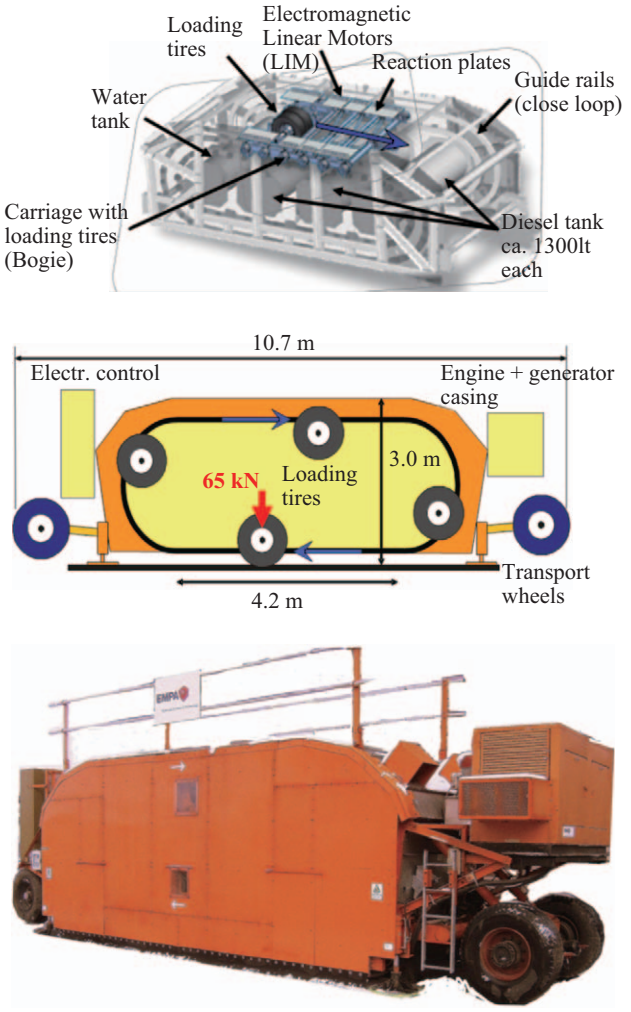

Fig. 18. Frame and detail of one of the bogies; schema of the loading principle; view of the MLS10.

The bogies are pulled contactless by 24 linear induction motors (LIM). The rails are built in such a way that the freely revolving tires touch down smoothly to the surface before loading the pavement along the trafficked path length.

The frame is enclosed by a noise reduction cover, confining all moving parts. The noise produced by the machine is approximately 83 dB, which is within tolerance for noise emissions from road transport during the day in Switzerland. In order to monitor the loads during trafficking, the dynamic movements of the suspension system are registered electronically and transferred via Bluetooth to a computer.

The MLS10 is equipped with four transport wheels which can be raised and lowered hydraulically, thus lifting up the whole frame by about 1m and giving room for maintenance work, such as checking tire pressures and pavement sensors as well as measurements of profiles together with crack and damage inspection. The transport wheels allow maneuvering of the machine around the test site and driving the MLS10 to or off low bed trucks for long distance transport. The possibility of easily transporting the MLS10 on a flatbed truck makes it fully mobile. A detail of the frame and bulk view of the MLS10 is presented in Fig. 18.

2. Use of MLS10 in Pavement Engineering

Pavement response and performance prediction is a highly complex issue. Failure of pavements occurs because of a deterioration that takes place gradually as a consequence of the accumulation of loading and/or the action of the environment on the materials, involving a huge amount of variables. With the MLS10, it is possible to simulate the repetitive action of a well-defined rolling wheel load of characteristics similar to real heavy vehicle trafficking in a compressed period of time. This allows to study different pavement structures in conditions that are comparable to reality.

Full-scale tests with a mobile load simulator can provide valuable information in several areas of pavement engineering, such as listed below:

- Evaluation of new pavement concepts (cold-mix or composite asphalt pavements).
- Optimization of the performance of multifunctional pavement concepts.
- Determination of the residual life of real in-service pavements in order to evaluate rehabilitation measures.
- Evaluation and comparison of the effect of different climate conditions on a similar pavement concept.
- Validation of dimensioning methods.

3. Example of Utilization of the MSL10

Thanks to its mobility, the MLS10 has been used in several testing sites in Switzerland and abroad. In some cases, the MLS10 was used to determine the endurance limit and residual bearing capacity of new and old pavements. It was mostly employed for testing flexible pavements with cement stabilized and unbound subbases, but was also used for testing slab and block pavements (Arraigada et al., 2012; Blab et al., 2012; Hugo et al., 2012). An example of how MLS10 is used to determine the lifespan and bearing capacity of a standard flexible pavement is presented as follows.

1) Objectives of the Tests

This example describes tests with the MLS10, focusing on the determination of the mechanical endurance limit of standard pavements for different traffic load classes through accelerated traffic simulation. Elaborate monitoring and theoretical calculations were used to determine the change of mechanical properties of the road under natural climatic conditions over the whole life time from new construction to complete loss of bearing capacity. The work provided a comparative basis for similar investigations with MLS10 regarding the endurance limit of innovative new pavements.

2) Studied Pavement

A new test section was built and loaded with the MLS10 until reaching the endurance limit. The pavement complies

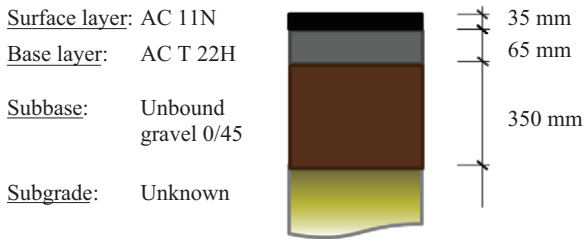

Fig. 19. Frame and detail of one of the bogies, schema of the loading principle view of the MLS10.

with a typical structure in the dimensioning catalogue of the Swiss standards (SN 640 324, 2011) where it is classified as a Type 1, T2, S2. This means that the subgrade was compacted until reaching the medium load bearing capacity category S2. The pavement structure was designed for a traffic load class T2 and consisted of two asphalt concrete layers (AC 11N and AC T 22H) on top of an unbound gravel 0/45 layer (Fig. 19).

3) Loading

The MLS10 was setup to apply 65 kN in each of the four bogies, using a super single tire configuration. This corresponds to half of a 130 kN axle load. The loads were calibrated using static scales. The tire pressure was set to 10.5 bar. The trafficking speed used for the tests was 22 km/h. The load was channelized, i.e. no lateral wandering was applied.

According to the design standard (SN 640 324, 2011) which is based on the AASTHO design guide (AASHTO 1986), the pavement is characterized by its structural number (SN) which is calculated considering the thickness of each of the layers of the pavement and the coefficient of bearing capacity (a) of the materials. Following the standard, it is possible to estimate a theoretical number of MLS10 load applications that will cause similar destructive effects than 20 years of traffic. The destructive effect of one 130 kN (13.26t) axle load, can be converted to the destructive effect of a reference load of 8.16t, by multiplying with an equivalent factor. This factor proposed by the standard suggests that the destructive effect of the MLS10 load configuration is 7.10 higher than the reference load. As a result, the expected total amount of reference loads tolerated by the newly constructed pavement in 20 years' service life, lies between the equivalent of 30'900 to 102'900 MLS10 load applications.

4) Instrumentation and Performance Evaluation

Deterioration of pavements is traditionally carried out by means of visual inspections, which provides a subjective assessment of road surface cracking or the development of ruts, among other types of distress. Moreover, devices which can be transported and used in different sections of a road can deliver an indication of the structural condition without producing damage. These devices usually measure the deflection of the surface. Different kinds of sensors are available for monitoring pavement deterioration over time. Strain gauges

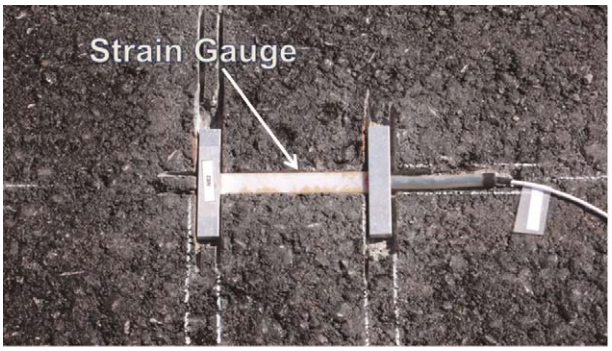

Fig. 20. Strain gauges, installation in the pavement.

and temperature sensors as well as weigh in motion sensors are common nowadays (Poulikakos et al., 2008; Poulikakos et al., 2010). However, installation and robustness of the sensors as well as data acquisition and interpretation are still a complex issue. In this investigation, the deterioration of the pavement was evaluated using the following tools:

Temperature sensors: Thermocouple wires were placed between the layers during construction of the pavement. These wires are for general purpose temperature measurements in asphalt, concrete and ambient air. They have Teflon insulation and can be used successfully without further protection in the paving process, even at high temperatures. Temperature was measured close to the wheel pass at the pavement surface and 3.5 cm and 10 cm below.

Strain gauges: For measuring the deformation of the pavement under load, gauges were embedded at different depths of the pavement. The installation of the sensors was carried out simultaneously with the construction of the pavement. They were placed in H shaped trenches prepared by cutting (Fig. 20) or by embedding wooden dummies in the hot mix asphalt during compaction. After finishing the compaction of the layers, the dummies were taken out and the sensors were placed into the trench. Six strain gauges were used: one between the base and subbase layers (10 cm below surface), perpendicular to loading direction and four between the surface and base layers (3.5 cm below the surface), along and perpendicular to loading direction; all of them under the tire. The last strain gauge was positioned on the surface, 46 cm from the center of the wheel path.

Accelerometers: In order to obtain the dynamic deflection of the pavement under the loading of the rolling tires, one accelerometer was installed close to the wheel path. Data acquisition was done simultaneously with the strain gauges and stored for post-processing analysis. More information on data analysis and interpretation can be found elsewhere (Arraigada et al., 2007; Arraigada et al., 2009).

Transversal profiles: Permanent deformation of the pavement surface was calculated by analyzing three profiles perpendicular to the trafficking direction. Measurements were carried out with the MLS profiler. Similar to the profilometer in Fig. 2, the profiler consists of a steel beam with a wheel on

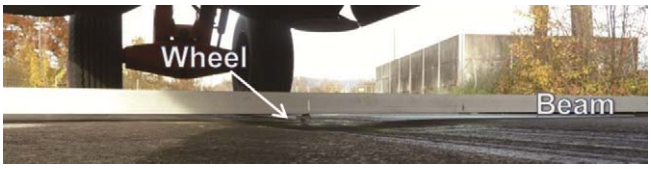

Fig. 21. View of the profiler used for rutting measurements.

Fig. 22. View of the Falling Weight Deflectometer (FWD) in testing position.

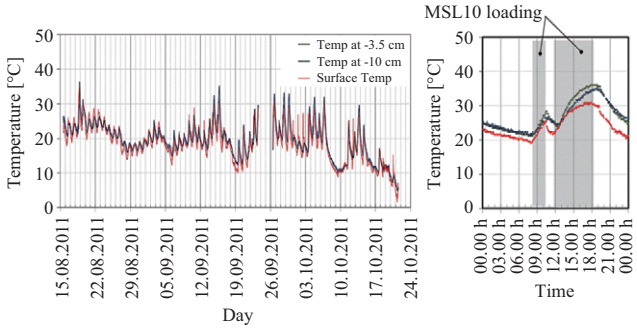

Fig. 23. Temperature recorded during the tests. On the right, the detailed temperature profile during one day.

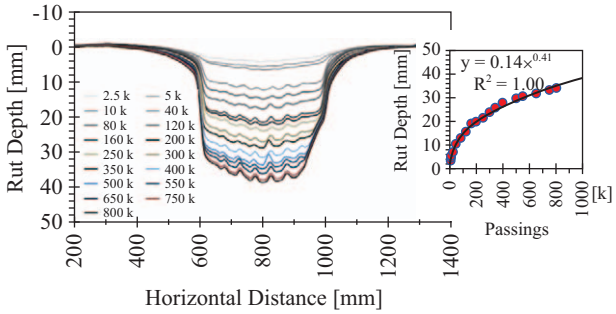

Fig. 24. Rutting profile and progressive rut depth *vs.* number of applications fitted with a power function.

the bottom side (see Fig. 21). For each measurement, the beam is placed on two steel plates that are glued to the pavement surface, outside the trafficked area, serving as "reference points". The beam distance to pavement can be set with a pair of adjustable feet at each end of the beam. This setup provides a stable frame for the measurements. A moving wheel situated in the bottom part of the beam travels in contact to the surface of the pavement, following any unevenness up to 1 mm. The combination of vertical and horizontal movement allows drawing the profile, which is expected to change throughout the tests due to permanent deformation. Consequently, measurements were taken periodically after a regular number of load applications in order to follow the increase of rutting *vs.* the accumulated number of loads.

Falling Weight Deflectometer (FWD): It consists of a trailer containing a mass and a line of geophones for measuring deflection. It can simulate the load of a passing truck by dropping a heavy weight on the pavement surface. The dynamic characteristics of the load are controlled with a spring element. The transient impulse load induces a deflection basin on the pavement surface, which is detected by a series of geophones in contact to the surface of the pavement. Surface velocities are recorded and converted to deflection. The amplitude and shape of the deflection obtained with this device are considered as indicator of the structural condition of the pavement. Two measurements, one before and after MLS10 loading were carried out following a grid of 45 measuring points, as shown in Fig. 22. From this grid, 5 points are in the loading path and the rest are in the non-loaded area. The back calculated elastic moduli of the pavement layers in each point were used to determine the change in the mechanical response due to the effect of loading, as explained later.

Visual inspection and forensic: The surface of the pavement was periodically inspected for detecting the formation and propagation of cracks. A photographic record over the loading history was performed systematically. Coring and trenching was carried out at the end of MLS10 loading.

5) Measurements Results

The temperature was measured continuously and a value was recorded every 5 minutes. Fig. 23 presents the temperatures during the 10 weeks of the tests. On the right, there is a detail of how is the temperature profile during one day when the MLS10 is loading the pavement. The gray shadowed areas mean that during that day, the machine loaded the pavement from early in the morning until late in the evening, with a stop of about 2 hour in the middle of the day. This shows that the temperature increases as a consequence of the repetitive loading of the machine, probably due to the internal friction generated by the deformation energy of the pavement.

Fig. 24 depicts the progressive surface deformation of the pavement with the accumulation of wheel passings. The colored lines show the relative total rutting at different loading times. The subfigure presents the evolution of the rut depth *vs.* the number of MLS10 wheel passings fitted with a potential

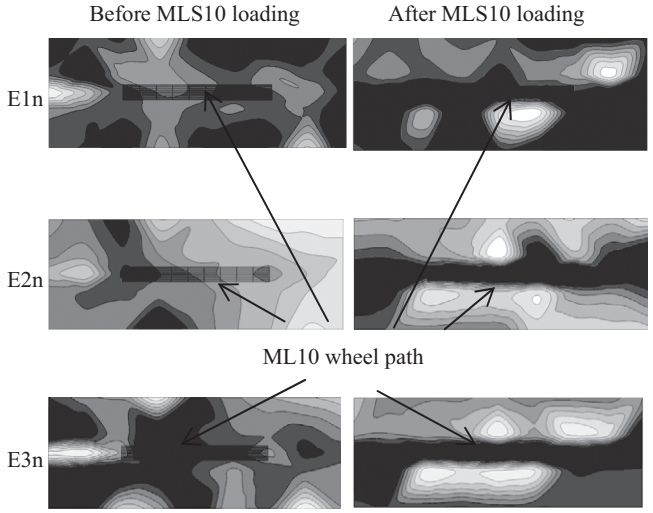

Fig. 25. Normalized elastic moduli before and after MLS10 loading (white low, black high modulus).

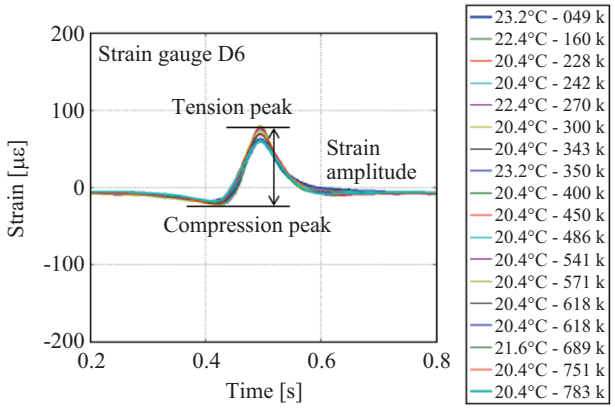

Fig. 26. Surface strains registered from a single load passing, at temperatures between 20°C-25°C and different number of load applications, indicated in the legend in thousands.

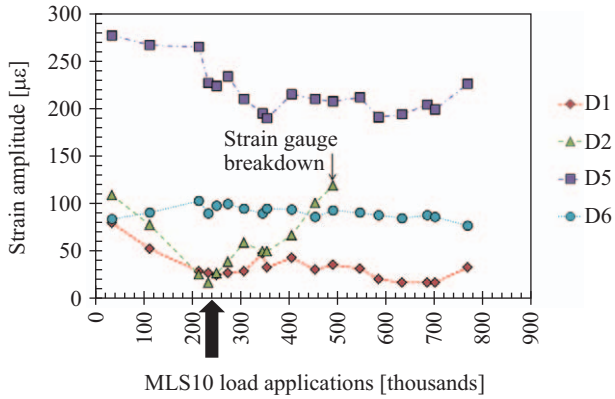

Fig. 27. Strains amplitudes *vs.* Nr. of MLS10 load applications for: Strain gauge D1, at -3.5 cm transversal to wheel path, Strain gauge D2, at -3.5 cm in wheel path direction, Strain gauge D5, at -10 cm transversal to wheel path, Strain gauge D6, at –surface, transversal, 46 cm from the wheel path.

function and coefficient of determination R^2. The shape of the rutting profiles confirms that the load was channelized and that rutting took place because of the settlement of the subgrade (no uplift along the sides of the rut). The profile further suggest that the MLS10 loading induced a post compaction of the unbound layers without shoving of the asphalt materials. In case of a road failure criterion of 20 mm rut depth, the pavement would have failed after 260'000 MLS10 wheel passings.

FWD measurements confirm that the subbase and subgrade layers suffered post-compaction just under the MLS10 loading path. Fig. 25 presents FWD results as normalized elastic modulus maps. To that end, the pavement structure was discretized in three parts 1, 2, 3, i.e.: the two bituminous layers as one layer, the subbase and the subgrade. The elastic moduli were back calculated as E1, E2 and E3 respectively. This was done for all points of the measuring grid.

Two measurement campaigns were carried out: one before and after finishing MLS10 loading. For each campaign, the back calculated values were normalized to the maximum elastic modulus of the measuring grid, giving as results E1n, E2n and E3n values that are positives numbers below or equal to 1. If the values are near to 1, means that the elastic modulus of the point in which the measurement was done is the highest in the measurement grid. Fig. 23 present the normalized elastic moduli of each layer, E1n, E2n and E3n as grey color maps. White color represent the lowest normalized elastic moduli, whereas black stand for values close to 1. The figure confirms that after MLS10 loading, the moduli of the subbase and subgrade layers E2n and E3n respectively, are highest under the wheel path due to local post-compaction.

Because of the viscoelastic nature of the asphalt, deformations and strains in the pavement are different with changing temperature or loading time. In order to analyze strain gauge data independently from loading characteristics, the loading parameters were kept constant throughout the course of the tests. However, since there was no temperature control, only records at similar temperatures were considered and compared. Fig. 26 shows records obtained in the transversal direction 46 cm away from the wheel track axis at the pavement surface. Each curve corresponds to a single MLS10 load passing, at similar temperatures (20°C to 25°C) but at different days, i.e. after different amount of accumulated MLS10 load applications (k = 1000). The strain amplitude induced by each load passing was calculated as the difference between the compression and tension peaks.

In Fig. 27, the strain amplitudes calculated from different strain gauges as previously explained are plotted *vs.* the number of MLS10 load applications. From the figure it can be observed, that due to the progressive compaction of the subbase and subgrade, the strains of the sensors D1 and D2 (at -3.5 cm) decrease until reaching a minimum at about 230'000 load applications (marked by an arrow). Afterwards, D1 displays transversal strain amplitudes that are about half of the

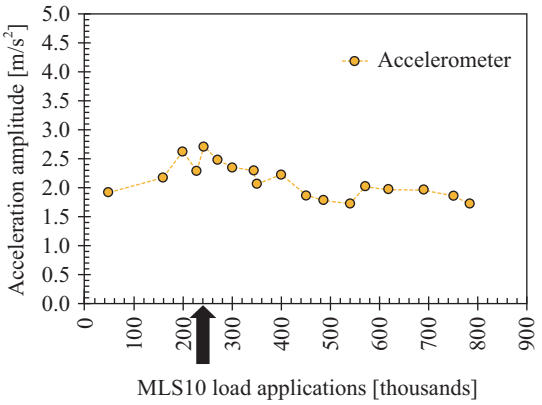

Fig. 28. Acceleration amplitudes *vs*. Nr. of MLS10 load applications.

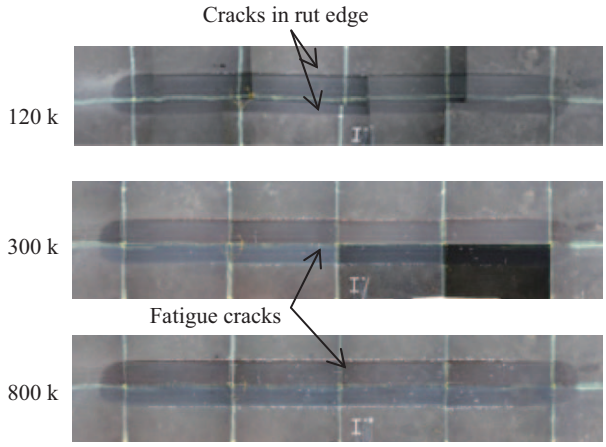

Fig. 29. Photographic record of the wheel path area after different amount of accumulated MLS10 load applications (in thousands).

initial ones. Similar performance can be observed for sensor D5 transversally positioned between the base and subbase layers. On the other hand, D2 increases until breakdown at 500'000 load applications indicating a loss of longitudinal stiffness due the initiation of cracking and interlayer debonding. The transversal strain amplitudes of gauge D6 are almost constant from the beginning until the end of the tests.

Acceleration records were evaluated considering that acceleration is the second derivative of displacement. In case of pavement deformation, the vertical displacement of the surface under loading is known as deflection. Plotting the acceleration amplitudes *vs*. the number of load applications results in Fig. 28. In this case, acceleration shows a moderate increase (i.e. reduction of deformation amplitudes) until about 230'000 MLS10 load applications, followed by a similar decrease, confirming results from strain gauge measurements.

Visual inspection showed that cracking of the surface occurred first on the rut edge, and started at around 120'000 MLS10 load applications. Between 200'000 and 300'000 load applications, the first random fatigue cracks appeared in wheel path, as shown in Fig. 29. These cracks propagated with the accumulation of MLS10 loadings. In some places, cracks

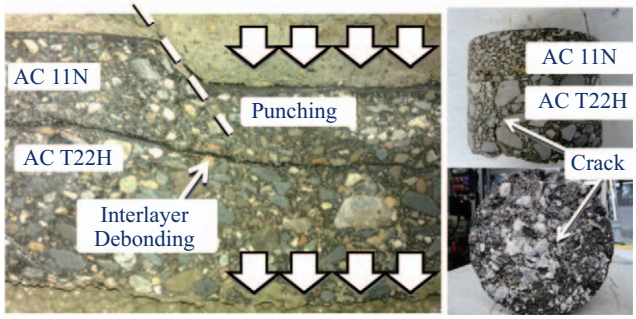

Fig. 30. View of a slab showing the deformation of the bituminous layers due to punching into the subbase and interlayer debonding. On the right, a core showing cracking on the bottom.

passed through all bituminous layers and the repeated pavement deflections caused pumping of fine aggregates from the subbase to the pavement surface.

Forensic studies confirmed that the bituminous layers punched into the unbound layers and due to the deformation showed interlayer debonding, as shown in Fig. 30. Moreover, several cores verified the existence of cracks on the bottom of the bituminous layers, caused by of the fatigue of the material.

IV. CONCLUSIONS

Some examples and applications of innovative applied asphalt testing and research with two special types of mobile accelerated traffic load simulators were presented.

The lower scale device MMLS3 proved successful for investigation adhesion of light reflectors and rutting of asphaltic plug expansion joints. It can be used in particular for determining rutting behavior of surface courses and fatigue behavior of thin flexible pavements under rolling wheel loads. The device proved particularly valuable in determining the water resistance of porous asphalt surface courses and in evaluation asphalt reinforcements in the laboratory. Tests can be conducted at a maximal environmental temperature of 45°C (climatic chamber or heated tent) or by heating up the road surface up to 60°C with a special fan consisting of two alternating flat nozzles.

From the test results for the reinforced pavements the performance against crack resistance of non-reinforced and glass grid reinforced laboratory slabs it became obvious that reinforced slabs have a higher resistance than non-reinforced slabs and that there are differences in the resistance for different glass grid reinforcements. For one glass grid reinforcement the resistance was 2 times for the other even 3 times higher than the resistance of the non-reinforced slab.

The different performance of the two reinforced slabs may be due to the fact that one grid had an additional polyester textile (felt) with a potentially negative impact on the bonding properties, leading to accelerated crack propagation and earlier failure. In case of reinforced slabs the crack propagation was delayed and when it appeared it eventually led to a delamination and debonding of the layers.

Thanks to the compact size and innovative design, the full-scale device MLS10 can be easily deployed to many places showing high flexibility and mobility. It can apply a high amount of heavy loads in a relatively short period of time. With a speed of 22 km/h and thanks to the unidirectional direction, the load is most similar to real traffic, compared to other mobile machines. The MLS10 allows the evaluation of new pavement concepts, the determination of the residual life of real in-service pavements and the validation of dimensioning methods.

The example showed that MLS10 was successful in generating complete loss of bearing capacity of a common standard pavement with realistic loads in only two months. The pavement response and failure mechanisms was successfully evaluated using a series of sensors, complemented with non-destructive tests and forensic studies.

According to the standards, the pavement was expected to reach the end of design life after an equivalent of 30'900 to 102'900 MLS10 load applications. Taking 20 mm as limit for acceptable pavement rutting, the experiment showed that 260'000 load applications were actually required, leading to the conclusion that the pavement was overdesigned. This was confirmed by measurements with strain gauges and accelerometers suggesting that severe cracking in the bottom took place after 230'000 load applications. Furthermore, visual inspection showed that surface cracking at the rut edges started after 120'000 load applications and surface fatigue cracking after ca. 200'000 to 300'000 load applications.

FWD measurements suggest that failure occurred because of densification of the unbound layers due to post-compaction. This was confirmed by forensic studies on a slab cut from the binder course and by the characteristic shape of the rut. The forensic study also showed that the extreme deformation cause interlayer debonding with cracks progressing from the bottom of the bituminous layers until eventually reaching the surface and allowing fine aggregates to be pumped up from the subbase. Finally, the results demonstrate the importance of creating a good bond between the layers in case of reinforcing flexible pavements confirming the suitability of the MMLS3 test setup for performance evaluation of pavement reinforcements in the laboratory.

REFERENCES

AASHTO-American Association of State Highway and Transportation Officials (1986). Guide for Design of Pavement Structures, Vol. 2, Washington D.C.

Arraigada, M., M. N. Partl and S. M. Angelone (2007). Determination of road deflections from traffic induced accelerations. Road Materials and Pavement Design 8(3), 399-421.

Arraigada, M., M. N. Partl, S. M. Angelone and F. Martinez (2009). Evaluation of accelerometers to determine pavement deflections under traffic loads. Materials and Structures 42(6), 779-790.

Arraigada, M., M. N. Partl and A. Pugliessi (2012). Initial tests results from the MLS10 mobile load simulator in Switzerland. Proceedings of the 4th international conference on accelerated pavement testing, Davis, CA, USA, 277-285.

Blab, R., W. Kluger-Eigl, J. Füssl and M. Arraigada (2012). Accelerated pavement testing on slab and block pavements using the mls10 mobile load simulator. Proceedings of the 4th international conference on accelerated pavement testing, Davis, CA, USA, 323-229.

Gubler, R., S. Küntzel and M. N. Partl (2004). Comparison of rutting behavior on test sections and circular test track using a model mobile load simulator. Proceeding of the 1st Int. Symp. on Design and Construction of Long Lasting Asphalt, ISAP, Auburn, USA, 1-14.

Hean, S. and M. N. Partl (2008). Eigenschaften von normalbreiten und überbreiten Fahrbahnübergängen aus Polymerbitumen nach starker Verkehrsbelastung (Behaviour of normal and wide asphaltic plug joints after heavy traffic loading). Eidgenössisches Departement für Umwelt, Verkehr, Energie und Kommunikation, Bundesamt für Strassen, AGB 2001(083), 627. (in German)

Hugo, F., M. Arraigada, L. Shuming, T. Zefeng and Y. R. Kim (2012). International case studies in support of successful applications of accelerated pavement testing in pavement engineering. Proceedings of the 4th international conference on accelerated pavement testing, Davis, CA, USA, 93-104.

Kim, H., K. Sokolov, L. D. Poulikakos and M. N. Partl (2009). Fatigue evaluation of carbon FRP-reinforced porous asphalt composite system using a model mobile load simulator. Transportation Research Record: Journal of the Transportation Research Board 2116, 108-117.

Partl, M. N. and S. Hean (2011). Experience with testing and performance evaluation of bituminous plug expansion joints on concrete road bridges. Int. J. of Roads and Airports 1(1), 1-17.

Poulikakos, L. D., M. Arraigada, G. C. J. Morgan, K. Heutschi, P. Anderegg, M. N. Partl and P. Soltic (2008). In situ measurements of the environmental footprint of freight vehicles in Switzerland. Transportation Research Part D: Transport and Environment.

Poulikakos, L. D., K. Heutschi, R. Muff, M. Arraigada, P. Soltic, P. Anderegg, M. N. Partl and P. Jordi (2010). Footprint II-Long term pavement performance and environmental monitoring on A1. Eidgenössisches Departement für Umwelt, Verkehr, Energie und Kommunikation, Bundesamt für Strassen, ASTRA 2005/009, Report 1288

Raab, C., M. N. Partl, K. Jenkins and F. Hugo (2005). Determination of rutting and water susceptibility of selected pavement materials using mmls3. Proceeding of the 7th Internat. Conference on the Bearing Capacity of Roads, Railways and Airfields, Trondheim, Norway, 1-10.

Raab, C. and M. N. Partl (2011). Stripping bei lärmmindernden Deckschichten unter Überrollbeanspruchung im Labormaßstab (Stripping of low noise surface courses during laboratory scaled wheel tracking). Eidg. Dept. für Umwelt, Verkehr, Energie und Kommunikation, Bundesamt für Strassen, VSS 2007/502, Report 1335. (in German)

SN 640 324 Schweizer Norm (Swiss Standard) (2011). Dimensionierung Strassenaufbaus, Unterbau und Oberbau (Dimensioning of road constructions, subgrade and pavement). Schweizerischer Verband der Strassen- und Verkehrsfachleute (VSS). (in German)

Sokolov, K., M. Stimolo, H. M. Burger and M. N. Partl (2005). Application of a model rutting tester for road safety installations. Materials and Structures 38(5), 533-540.